ACCOUNTS of chemical research

Article

pubs.acs.org/accounts

Reactions of HNO with Metal Porphyrins: Underscoring the Biological Relevance of HNO

Fabio Doctorovich,*[,‡] Damian E. Bikiel,[‡] Juan Pellegrino,[‡] Sebastián A. Suárez,[‡] and Marcelo A. Martí*[,‡,†]

[‡]Departamento de Química Inorgánica, Analítica y Química Física/INQUIMAE-CONICET and [†]Departamento de Química Biológica, Facultad de Ciencias Exactas y Naturales, Universidad de Buenos Aires, Ciudad Universitaria, Pab. II (1428), Buenos Aires, Argentina

CONSPECTUS: Azanone (^{1}HNO, nitroxyl) shows interesting yet poorly understood chemical and biological effects. HNO has some overlapping properties with nitric oxide (NO), sharing its biological reactivity toward heme proteins, thiols, and oxygen. Despite this similarity, HNO and NO show significantly different pharmacological effects. The high reactivity of HNO means that studies must rely on the use of donor molecules such as trioxodinitrate (Angeli's salt). It has been suggested that azanone could be an intermediate in several reactions and that it may be an enzymatically produced signaling molecule. The inherent difficulty in detecting its presence unequivocally prevents evidence from yielding definite answers. On the other hand, metalloporphyrins are widely used as chemical models of heme proteins, providing us with invaluable tools for the study of the coordination chemistry of small molecules, like NO, CO, and O_2. Studies with transition metal porphyrins have shown diverse mechanistic, kinetic, structural, and reactive aspects related to the formation of nitrosyl complexes. Porphyrins are also widely used in technical applications, especially when coupled to a surface, where they can be used as electrochemical gas sensors. Given their versatility, they have not escaped their role as key players in chemical studies involving HNO.

This Account presents the research performed during the last 10 years in our group concerning azanone reactions with iron, manganese, and cobalt porphyrins. We begin by describing their HNO trapping capabilities, which result in formation of the corresponding nitrosyl complexes. Kinetic and mechanistic studies of these reactions show two alternative operating mechanisms: reaction of the metal center with HNO or with the donor. Moreover, we have also shown that azanone can be stabilized by coordination to iron porphyrins using electron-attracting substituents attached to the porphyrin ring, which balance the negatively charged NO^-.

Second, we describe an electrochemical HNO sensing device based on the covalent attachment of a cobalt porphyrin to gold. A surface effect affects the redox potentials and allows discrimination between HNO and NO. The reaction with the former is fast, efficient, and selective, lacking spurious signals due to the presence of reactive nitrogen and oxygen species. The sensor is both biologically compatible and highly sensitive (nanomolar). This time-resolved detection allows kinetic analysis of reactions producing HNO. The sensor thus offers excellent opportunities to be used in experiments looking for HNO. As examples, we present studies concerning (a) HNO donation capabilities of new HNO donors as assessed by the sensor, (b) HNO detection as an intermediate in O atom abstraction to nitrite by phosphines, and (c) NO to HNO interconversion mediated by alcohols and thiols.

Finally, we briefly discuss the key experiments required to demonstrate endogenous HNO formation to be done in the near future, involving the *in vivo* use of the HNO sensing device.

INTRODUCTION

Interest in HNO (azanone according to IUPAC; usually nitroxyl) has increased in the past decade due to its remarkable chemical properties and increasing biological relevance.[1] HNO displays a unique spin-forbidden acid−base equilibrium[1] (^{1}HNO ↔ $^3NO^-$ + H^+; pK_a = 11.4), and is intrinsically unstable due to a fast dimerization yielding nitrous oxide (2HNO → H_2O + N_2O; k_{dim}= 8 × 10^6 M^{-1} s^{-1}).[2] These properties make handling of HNO difficult, and it must be produced *in situ* from HNO donors; this adds to the challenge of time-resolved direct detection and quantification. Several pharmacological studies have shown that the effects of HNO are distinct from those of nitric oxide (NO). HNO causes preferential venous dilation, whereas NO affects both arterial and venous smooth muscle.[3] However, because their signaling pathways are not completely differentiated, it could be that many biological functions that are attributed to NO are really promoted by HNO. In fact, NO/HNO interconversion is still a fundamental open question, and providing a definite answer to this issue is an extremely difficult task. Evidence for positive effects of HNO in preventing heart failure were also reported,[1] which results in a strong motivation for the development of HNO prodrugs for therapeutic applications. Last, but not least, routes for HNO endogenous production have been also suggested, such as production by nitric oxide synthase (NOS)

Received: April 15, 2014
Published: September 19, 2014

   dx.doi.org/10.1021/ar500153c | *Acc. Chem. Res.* 2014, 47, 2907−2916

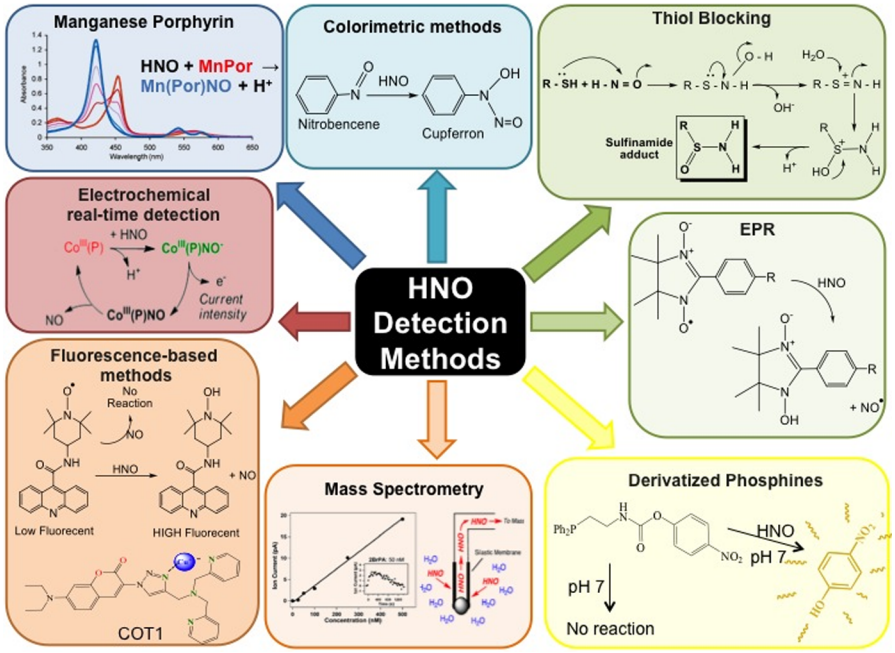

Figure 1. HNO detection methods.

under restrictive conditions,[1,4] among other RNOS redox related reactions.[5] Still, evidence for the endogenous formation of azanone in living organisms has not been reported, possibly due to the inherent difficulties associated with its unequivocal detection.

In order to understand the chemical biology of azanone, a better knowledge of its complex reactivity is needed. HNO biological targets are mainly metal complexes, proteins, thiols, NO, and dioxygen. Therefore, significant overlap with the reactivity of NO is observed, and predicting the actual fate of azanone requires careful determination of the rate and products of each and every reaction. As an example, heme proteins have been shown to react with HNO and NO in both the Fe(III) and Fe(II) states,[6,7] yielding in the latter case a stable $Fe^{II}P$–HNO adduct (P = heme).[8] Several studies have been performed on the reaction of azanone with Mn, Fe, and Co porphyrins,[9−14] showing interesting features concerning the underlying mechanism, rate, and selectivity. Particularly exciting is the use of a Co(III) porphyrin immobilized on a gold surface as an electrochemical method for selective azanone quantification, allowing the time-resolved concentration of HNO to be determined down to the nanomolar level.[15]

In the past decade several direct HNO detection and quantification methods have emerged (Figure 1).[1,16−21] Previously, methods relied on indirect evidence of HNO by detection of its reaction products, such as N_2O. Strategies for direct detection are diverse: the use of thiols as trapping agents followed by HPLC analysis;[18,22−24] spectroscopic methods based on HNO reaction with metal complexes,[9,11,14,19] such as fluorescence[20,21,25] or reaction with phosphines,[17] and even EPR[1,26] and mass spectrometry.[16] These sensing techniques have triggered the study of a number of reactions involving HNO, under a variety of circumstances (including in living cells) and with high sensitivity (up to the nanomolar level), and it can be envisioned that in the future these could be of help in answering some of the fundamental questions related to the chemical biology of HNO, such as: is azanone produced endogenously? If so, how and where is it produced? Are some of the biological signaling pathways nowadays attributed to NO due to HNO? Could it be a product of NO interconversion or is it the other way around? Or both? We hope that answers to these questions will soon be found along with a greater appreciation of the chemical and biological importance of HNO.

It should be noted that $E°(NO/^3NO^-) = -0.81$ V[1] and $E°(NO^•, H^+/HNO) = -0.11$ V,[2] becoming −0.55 V at pH 7 (all values against NHE). This last value is around the limit for biological reducing agents. However, it has to be taken into account that prediction of reaction feasibility by using its ΔE value only applies under equilibrium, at the pH values and concentrations at which the reduction potentials were calculated, and for outer sphere electron transfer mechanisms.

■ HNO/NO⁻ IRON COMPLEXES

$\{FeNO\}^n$ complexes with n = 6, 7, and 8 are key intermediates in NO and nitrite-reducing enzymes in bacteria and fungi, which catalyze important processes related to the biogeochemical cycle of nitrogen. $\{FeNO\}^n$ is the notation proposed by Enemark and Feltham in recognition of the covalent nature of the M−NO bond, where n stands for the number of electrons in the metal d and NO π^* orbitals.[27] By use of a simplified limiting approach, the $\{FeNO\}^{6/7/8}$ complexes can be described as an iron(II) center coordinated to NO^+, $NO^•$, or NO^-/HNO, respectively. Initially, Enemark and Feltham did not include the HNO complexes in their formalism since its main goal was to extend Walsh's molecular orbital diagrams for triatomic species to understand the MNO angles in nitrosyl complexes. However, since HNO complexes are simply protonated NO^- complexes, it seems reasonable to classify them as $\{MNO\}^8$ complexes.

Recently, an increasing number of reports on $\{FeNO\}^8$ complexes have contributed to the spectroscopic characterization of this initially elusive species, but still much more investigation is needed to elucidate mechanistic issues. An interesting example is the catalytic cycle of fungal nitric oxide reductase (P450nor), which converts NO to N_2O via a

dx.doi.org/10.1021/ar500153c | Acc. Chem. Res. 2014, 47, 2907−2916

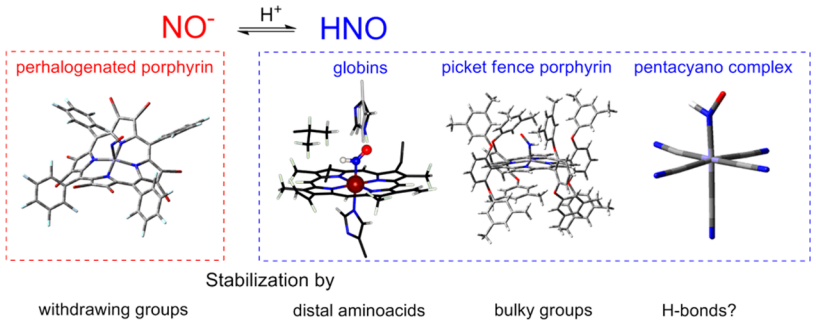

Figure 2. Different platforms for stabilizing NO^-/HNO iron complexes.

proposed $\{FeNO\}^8$ intermediate (intermediate I); this then reacts with NO to generate N_2O and the Fe(III) form.[28] The first spectroscopic evidence of the existence of $\{FeNO\}^8$ heme model complexes were obtained from spectroelectrochemical experiments with $Fe^{II}PNO$ (P = TPP and OEP).[29,30] The reaction of $[Fe^{II}PNO]^-$ with weak acids was also studied; the protonated HNO complex was not stable and oxidized back to the $\{FeNO\}^7$ complex.[30] In the electrocatalytic reduction involving the water soluble porphyrin $[Fe(TSPP)]^{3-}$, nitrite is reduced to ammonia as in the case of nitrite reductases, through the intermediacy of $\{FeNO\}^{6-8}$ species, which were also proposed in theoretical papers.[31]

We have focused on using electron-poor porphyrins to stabilize $\{FeNO\}^8$ complexes because of their importance in bioinorganic chemistry and because all previously reported $\{FeNO\}^8$ heme models have proved impossible to isolate due to their susceptibility to oxidation.[29,30] The $\{FeNO\}^8$ complex $[Co(C_5H_5)_2]^+[Fe(TFPPBr_8)NO]^-$ was obtained from reduction of the $\{FeNO\}^7$ complex $Fe^{II}(TFPPBr_8)NO^\bullet$ with cobaltocene, and according to spectroscopic and theoretical evidence, its electronic structure was assigned as intermediate between $Fe^{II}NO^-$ and $Fe^{I}NO^\bullet$,[32] in contrast with the predominant $Fe^{II}NO^-$ character of previous reports of *non-heme* $\{FeNO\}^8$ complexes.[33] In fact, biologically relevant non-heme $\{FeNO\}^8$ complexes, implied in bacterial NO reductases, are high-spin with an $S = 1$ ground state.[34] The ^{15}N NMR spectrum, never reported before for an $Fe^{II}NO^-$ system, showed irrefutable evidence of a diamagnetic deprotonated $\{MNO\}^8$ complex, with a signal at +790 ppm vs $CH_3{}^{15}NO_2$, a value in the upper limit of previously characterized $\{MNO\}^8$ complexes. The use of electron-withdrawing groups on the porphyrin ring enhanced stability with respect to earlier studied systems. The reduction of the $\{FeNO\}^7$ system showed a second reversible wave in the CV, and this second reduction product, $[Fe(TFPPBr_8)NO]^{2-}$, was also characterized by FTIR and UV–vis spectra in solution.[35] Although, in principle, a somewhat larger degree of reduction on NO is expected, the N–O stretching IR band shifted from 1550 to 1590 cm^{-1} (the opposite trend would be expected for augmented electron density on the FeNO moiety). This increase in the N–O stretching frequency was predicted by DFT calculations not for the low spin complex (S =1/2), but for the intermediate or high spin states (S = 3/2 or 5/2). The Fe–N–O angle in the calculated structures of these states is similar to the $\{FeNO\}^7$ complex; this and the higher N–O stretching frequency suggested the structure $[\{FeNO\}^7(TFPPBr_8{}^{4-})]^{2-}$ for the doubly reduced product.

While the perhalogenated porphyrin resulted an appropriate platform to stabilize the $FeNO^-$ moiety, attempts to protonate $[Fe(TFPPBr_8)NO]^-$ to give the expected Fe(P)HNO complex were unsuccessful, yielding instead the $\{FeNO\}^7$ complex. Although isolated iron porphyrins seemed unable to present stable *protonated* $\{FeHNO\}^8$ complexes, a fairly stable $\{RuHNO\}^8$ complex, [Ru(TTP)(HNO)(1-MeIm)], was obtained without the support of a protein environment, suggesting an additional source of stabilization of the HNO–porphyrin moiety.[36] Note that the only well characterized heme $\{FeHNO\}^8$ complexes known to date were prepared in the myoglobin active site and with human, soy, and clam hemoglobin. In these systems, the distal residues may play a crucial role in the stabilization of the protonated adduct.[8,37]

Interestingly, recent results show the use of a picket-fence porphyrin, which allows formation of the protonated Fe(P)-HNO complex by reaction of the NO^- complex with acetic acid.[38] The HNO complex also decomposes to a $\{FeNO\}^7$ complex but at a slower rate (90% after 20 h). However, the underlying reason for the instability of the $\{FeHNO\}^8$ complex relative to the disproportion to $\{FeNO\}^7$ and H_2 is not clear. The non-heme $\{FeHNO\}^8$ complex $[Fe(CN)_5(HNO)]^{3-}$ has been reported as a stable $Fe^{II}HNO$ complex in aqueous solutions;[39] in the pentacyano platform, we can neither invoke the supplied stabilization by amino acids as in the protein complexes nor the steric protection provided by the bulky substituents in the picket fence adduct. Clearly there are other factors influencing the stability of the $\{FeHNO\}^8$ moiety, for example, stabilization through hydrogen bonds with the solvent. Figure 2 summarizes the stable FeHNO complexes reported so far.

HNO TRAPPING BY METALLOPORPHYRINS

The reactions of HNO with metalloporphyrins (MP) of iron, manganese, and cobalt were interesting targets for investigation due to the reactivity of HNO and NO toward heme proteins, and the many known reactions of NO with metalloporphyrins forming stable ferrous nitrosyl adducts.[9,10,15] The interactions of the HNO donors sodium trioxodinitrate (AS, Angeli's salt) and toluenesulfohydroxamic acid (TSHA, a Piloty's acid (PA) derivative) with Fe(III)P (both in water and in organic media) were studied.[9] As expected, we observed efficient conversion to the corresponding nitrosyl adduct, $\{FePNO\}^7$. The reaction was easily followed by UV–vis spectroscopy, despite the slight spectral changes. Following the observed success, we tested Mn(III)P, which, as their iron analogues, showed efficient conversion to the corresponding $\{MnNO\}^6$ adducts upon exposure to both HNO donors. Interestingly, MnPNO showed a significant shift in the Soret band (>30 nm) with respect to the MnP reactant, providing the foundations for a colorimetric HNO detection assay.[10]

dx.doi.org/10.1021/ar500153c | *Acc. Chem. Res.* 2014, 47, 2907–2916

Our analysis in the reaction kinetics of these systems reveals two different behaviors related to the rate of nitrosyl–porphyrin production and the stoichiometric donor/porphyrin ratio required to convert Fe(III)/Mn(III) porphyrins. When negatively charged porphyrins reacted with AS (pH 7) or PA (pH 10), a large excess of donor was required to drive the reaction to completion (see Figure 3). Equimolar ratios led to half-lives on the order of 100 min. In contrast, positively charged porphyrins (TEPyP) used in an equimolar ratio went to completion with half-lives of seconds.

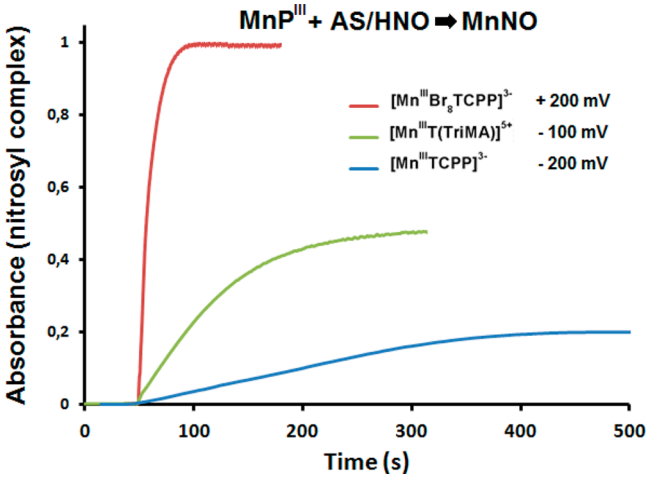

Figure 3. Absorbance, λ_{max}, corresponding to the peak position of each nitrosyl complex vs time plot, for the reaction of three $Mn^{III}P$ (1×10^{-5} M) with Angeli's salt (AS; 5×10^{-5} M) in phosphate buffer (0.1 M) at 25 °C (reduction potentials are indicated in the plot).

A direct porphyrin–donor interaction is suggested because the effective nitrosyl porphyrin formation rate by far exceeds the donor spontaneous decomposition, the reaction is first order dependent on donor concentration, and these porphyrins accelerate donor decomposition. For slower reactions that do not show a linear rate vs donor concentration relationship, the expected spontaneous generation by the donor and subsequent azanone reaction with the porphyrin was assumed to be the operative mechanism.

By measuring the nitrosyl formation rate, d[MPNO]/dt, as a function of initial donor concentration, we determined the porphyrin–donor association bimolecular rate constants ($k_{onDonor}$) for the *fast* cases or the porphyrin–HNO association bimolecular rate constants (k_{onHNO}) for the *slow* cases (see Figure 4). The overall mechanism is presented in Scheme 1.

During the past decade, we have determined the rates for the reactions of the HNO donors AS and TSHA with several water-soluble Mn and Fe porphyrins differing in their total peripheral charge (positive, neutral, or negative) and redox potentials (reducing, that is, with $E° < 0$ mV, or oxidizing, with $E° > 0$ mV). These results are summarized in Figure 4.

The results presented in Figure 4 show that for all MnP the same k_{onHNO} values are obtained either with AS and TSHA, while a narrow distribution of values is also obtained for $k_{onDonor}$. Considering the redox potential, it is clear that those MnP showing a positive redox potential (>100 mV), accelerate donor decomposition, despite their peripheral charge. Conversely, MnP complexes showing a negative redox potential (less than −160 mV) trap free HNO.[41] DFT studies suggest that the catalytic effect can be understood either in terms of a redox reaction, which results in reduced porphyrin and oxidized donor followed by rapid decomposition to NO and combination to yield a nitrosyl complex (MPNO), or by direct

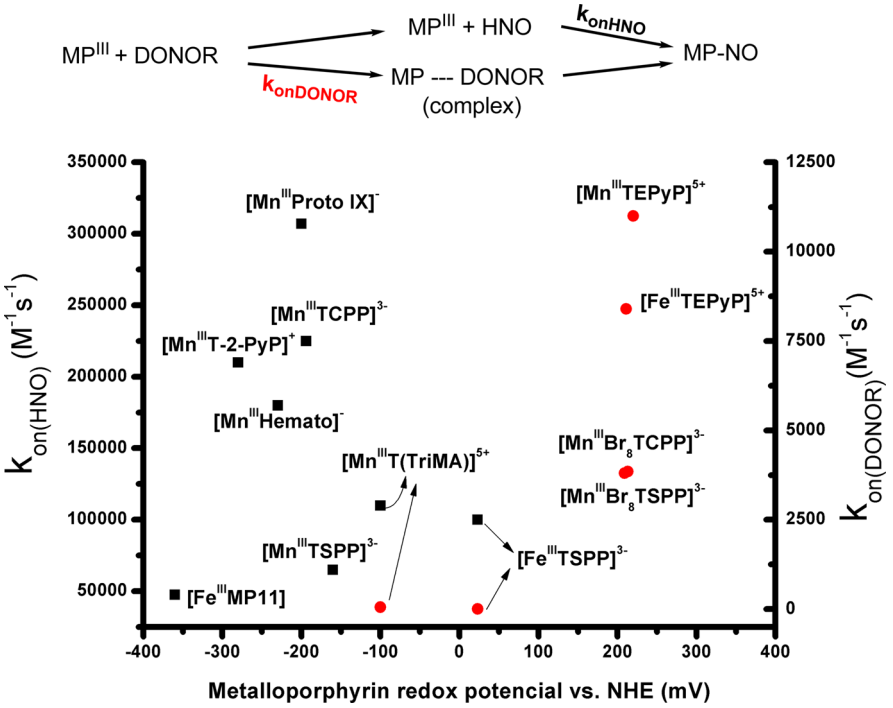

Figure 4. Values of k_{on} (M^{-1} s^{-1}) for HNO trapping (black, left axis) and donor trapping (red, right axis) by Fe and Mn porphyrins. Metalloporphyrins with $E < -100$ mV[40] trap HNO, while those with $E > -100$ mV[40] react with the donor. Porphyrins with $E \approx -100$ mV[40] react by both pathways.

dx.doi.org/10.1021/ar500153c | *Acc. Chem. Res.* 2014, 47, 2907–2916

Scheme 1. Two Different Reaction Mechanisms between Metalloporphyrins and Common HNO Donors[a]

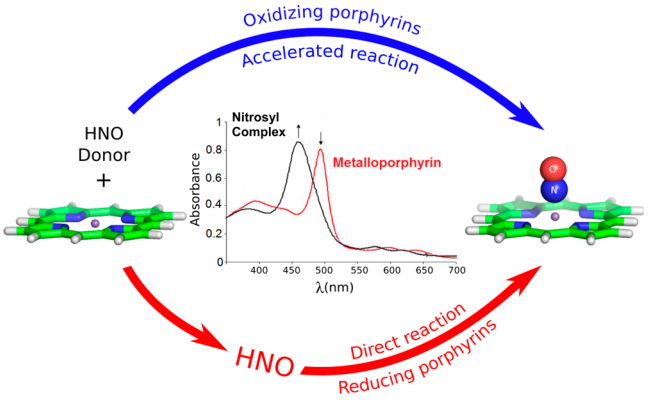

[a]In blue is the accelerated mechanism, where the porphyrin–donor association bimolecular rate constants were measured. In red is the direct reaction mechanism, where the first step is the donor decomposition to generate HNO and HNO reacts with the porphyrin in a second step.

coordination of the donor to the metal that promotes X–NO bond breakage.[41]

Another particularly interesting point that arises as a global picture concerns the fact that even if myoglobin–HNO adducts and $FePNO^-$ complexes have been obtained, no reaction is observed with either PA or AS for any of the studied iron porphyrins in the ferrous state. Thus, while NO is promiscuous for both Fe(III) and Fe(II), HNO is selective for ferric porphyrins. The same observation was made for Mn porphyrins. Only Mn(III) reacts with azanone. CoP behaves similar to MnP: Co(III)P efficiently reacts with azanone donors to produce the corresponding nitrosyl, being inert to NO, and Co(II)P reacts with NO but not with HNO. According to our data and previous works, it is clear that AS or PA (or HNO) does not react with ferrous porphyrins, or that the ferrous–HNO complex, if established, is not stable and does not accumulate to allow spectroscopic detection. Although we do not know the reason underlying this behavior, it seems likely that the potential ferrous–HNO complex is too labile (i.e., HNO dissociation exceeds the rate of HNO binding), and thus no complex is observed without the presence of the protein matrix to stabilize it (as seen in several globins). The differential reactive behavior with NO/HNO for each MP is summarized in Scheme 2. It clearly shows that while Mn and Co porphyrins can distinguish between NO and HNO based on their redox states, Fe(III) analogues react with both species in both redox states and cannot be used for discrimination purposes.

Combining all available data, it is possible to perform a comparative analysis for the reaction kinetics of NO and HNO with metalloporphyrins and heme proteins (Table 1). The results shows that HNO association rate constants to M(III)P and ferric heme proteins fall in the 5×10^4 to 1×10^6 M^{-1} s^{-1} range, being similar to the values obtained for NO binding to ferric hemes. These rates are *ca.* 1000 times smaller than those for NO (or CO) binding to ferrous hemes. This can be explained by the fact that in ferric hemes the ligand association rate is limited by water release, while in ferrous hemes, the coordination site is empty.

Table 1. HNO and NO Binding Constant to Ferrous and Ferric Heme Proteins and Other Heme Models

target	$E_{1/2}$ vs NHE (mV)	reactant	k_{on} (M^{-1} s^{-1})	ref
Fe^{III}MP11	−280	HNO	3.1×10^4	11
		NO	1.1×10^6	42
$[Fe^{III}TSPP]^{3-}$	+23	NO	4.5×10^5	43
$[Fe^{II}TSPP]^{4-}$	−300	NO	1.5×10^9	43
Cyt-c(Fe^{III})	+250	HNO	4×10^4	44
catalase(Fe^{III})	−226	HNO	3×10^5	44
metMb(Fe^{III})	+120	HNO	8×10^5	44
Mb(Mn^{III})	−320	HNO	3.4×10^5	14
Mb(Fe^{II})	−430	HNO	1.4×10^4	45
		NO	2.0×10^7	46
O_2		HNO	3×10^3	44

Scheme 2. HNO versus NO Reactivity of Mn, Co, and Fe Porphyrins and UV-Vis Shifts of the Soret Bands for the Corresponding M(P)NO Products[1,9,10,12]

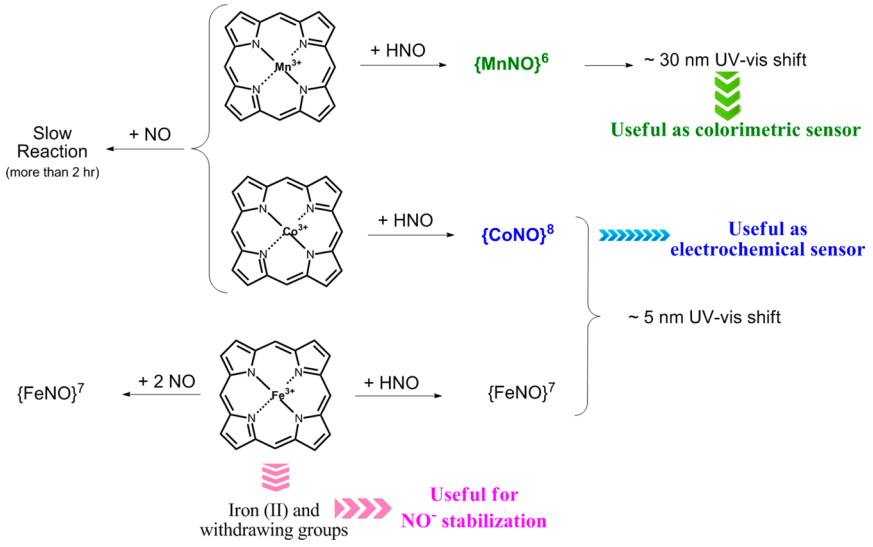

dx.doi.org/10.1021/ar500153c | Acc. Chem. Res. 2014, 47, 2907–2916

TIME-RESOLVED SELECTIVE ELECTROCHEMICAL DETECTION OF HNO

In vivo measurement of HNO requires a small device (millimeter or smaller) capable of functioning in aqueous solution. Using our knowledge of the chemistry of HNO with metalloporphyrins and due to their widespread use in electrochemical applications, we have developed an electrochemical HNO sensor.[15] After several preliminary tests in solution, a cobalt (II) porphyrin provided with four sulfur anchors [Co(P)], which can be covalently immobilized on gold electrodes, was selected (Figure 5). The electrode showed good

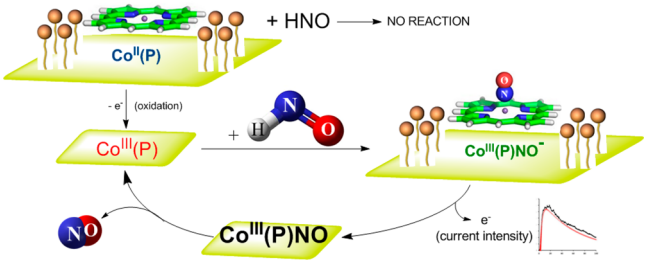

Figure 5. Mechanism of electrochemical HNO detection by Co(P) covalently attached to a gold surface.

selectivity toward azanone, being able to form stable $Co^{III}(P)$-NO^- adducts through the reaction of Co^{III} with HNO donors. The remaining surface was covered with cysteamine ($HSCH_2CH_2NH_2$), rendering it inert to NO.

In the amperometric detection of HNO (Figure 5), the electrode resting state is set to 0.8 V, where the porphyrin is stable in the $Co^{III}(P)$ state and no current is observed. The presence of HNO results in formation of the $Co^{III}(P)NO^-$ adduct, which under these conditions is oxidized. The resulting $Co^{III}(P)NO$ releases NO completing the cycle. The current intensity is proportional to the amount of HNO that binds to Co(P). Figure 6A shows the current intensity versus time plots after the addition of the HNO donor. A few seconds after the addition, a steep rise in the signal is observed; the maximum increases with donor concentration. A slow decay is then observed; similar to the donor spontaneous decomposition rate. A kinetic model was developed to allow us to analyze the current intensity versus time profiles. This model assumes the presence of a thin diffusion layer close to the electrode surface allowing us to directly relate the current intensity with the bulk HNO concentration through a system-dependent effective rate. This scheme can be used to determine the kinetics of HNO-related reactions as shown in the next section. Figure 6b shows simulated and measured current intensity showing the excellent agreement of our kinetic model.

To determine the electrode sensitivity and dynamic range, we performed an independent estimation of bulk HNO concentration and its relation to the observed peak current intensity (ΔC). We estimated the bulk HNO concentration at its peak by measuring the Mn nitrosyl porphyrin production rate under the same conditions as those used with the electrode and also using a simplified kinetic model.

Figure 7 shows the peak current (ΔC) as a function of bulk HNO concentration, showing that the electrode has a linear

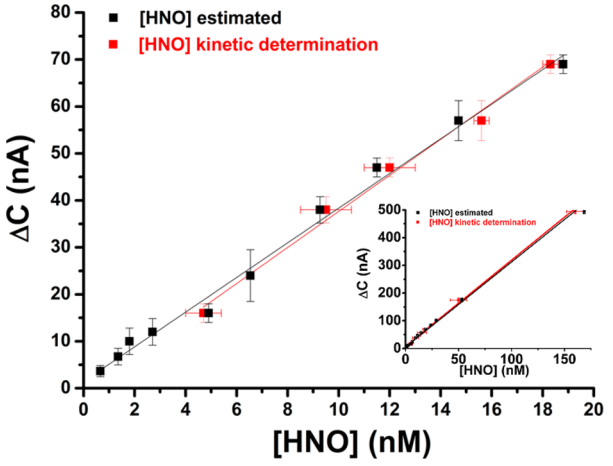

Figure 7. Electrode calibration of the current intensity as described in ref 12. The HNO concentration range is *ca.* 1−20 nM. Inset: The same as above for HNO concentration range of *ca.* 1−150 nM.

response in the 1 nM to 1 μM range allowing us to quantify azanone at nanomolar concentrations. An analysis of the electrode response in the presence of other reactive nitrogen and oxygen species (RNOS) in a complex biological media showed that although the electrode response is affected, it can still detect HNO at nanomolar levels. The most dramatic effect

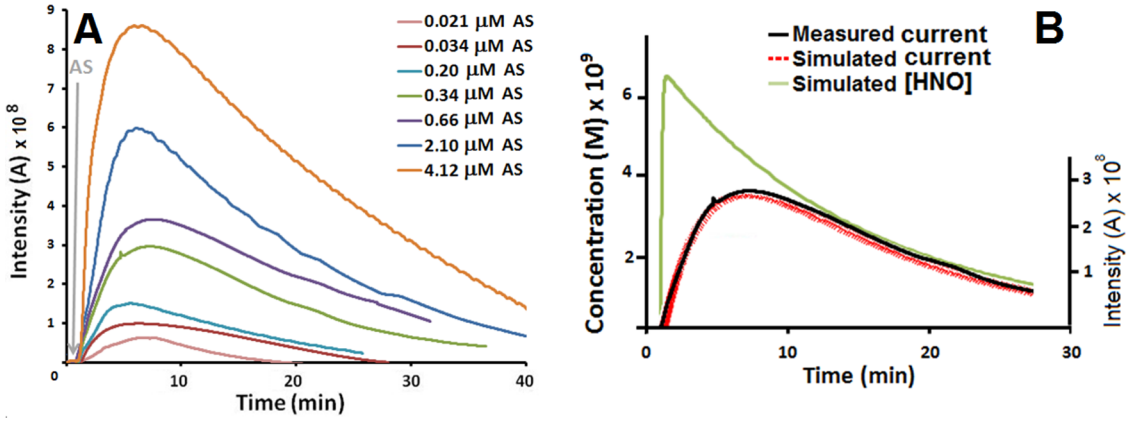

Figure 6. (A) Current intensity versus time plots for Co(P) modified electrode after the addition of increasing concentrations of HNO donor (AS). (B) Measured and simulated current vs time (black and red, respectively, right axis), and simulated HNO concentration at the same donor concentration (0.34 μM, green, left axis). A slight delay is observed in the signal.

dx.doi.org/10.1021/ar500153c | *Acc. Chem. Res.* 2014, 47, 2907−2916

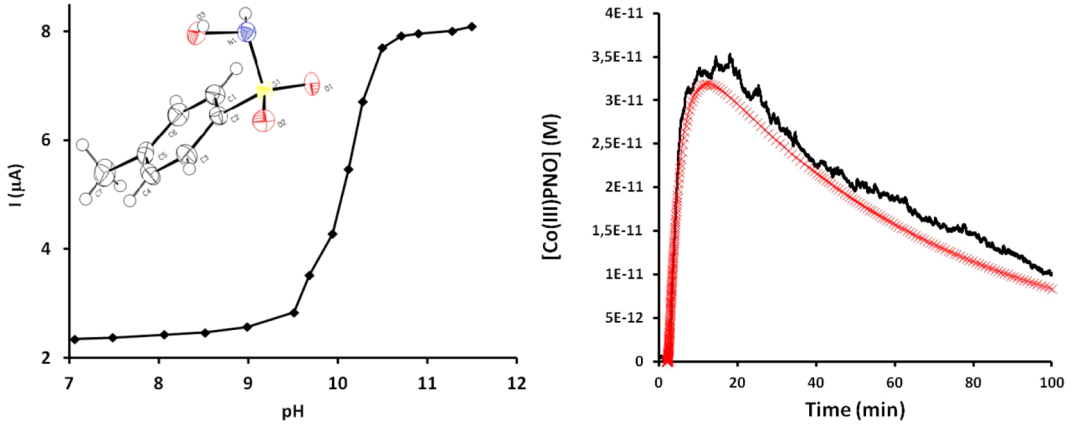

Figure 8. (left) pH versus current intensity for Me−PA. The current can be converted to HNO concentration as previously described.[15] (right) Time-resolved electrode response for a 3.4 μM solution of Me−PA (black) and simulated (red).

on the electrode signal is due to the presence of oxygen. The electrode response in cell culture with intact cells and with lysed cells is only minimally altered.

APPLICATIONS OF THE HNO-SENSING ELECTRODE

The sensor allows us to systematically probe for the presence of HNO in practically any chemical or biological reaction. Our first application was to use it to analyze HNO donation for a set of *N*-hydroxy-benzenesulfonamides, that is, PA-like derivatives that include electron-withdrawing and -donating substituents (Scheme 3).

We measured the peak current intensity vs pH (Figure 8A), which allowed determination of the optimal pH range of HNO production.[47] Kinetic measurement of the intensity (proportional to HNO concentration) versus time plots yielded the donor decomposition rate constant (Figure 8B).[15]

Comparison of the properties for all donors, in terms of rate and pH range of HNO release (Table 2), showed that

Scheme 3. HNO Releasing N-Hydroxy-benzenesulfonamide Derivatives

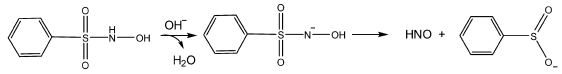

Benzenesulfonamide	Abbreviation	R_1	R_2	R_3
N-hydroxy-4-methyl	Me – PA	H	H	Me
N-hydroxy-4-nitro	NO_2 – PA	H	H	NO_2
N-hydroxy-4-Fluoro	F – PA	H	H	F
N-Hydroxy-2,4,6-triisopropyl	Triiso - PA	IsoP	IsoP	IsoP
N-hydroxy-4-methoxy	OMe – PA	H	H	OMe
N-hydroxy-2-nitro-4-trifluoromethyl	(NO_2-CF_3) – PA	H	NO_2	CF_3

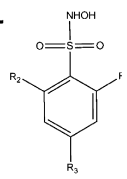

significant differences are observed and that the fluorinated and triiso derivatives release HNO *c.a.* 10 times faster than PA, and in a physiologically compatible pH range.

The second opportunity to test the electrode performance was in collaboration with Ford's group[48] in the context of oxygen atom transfer reaction studies from nitrite to a water-soluble phosphine (tppts) and biological thiols, mediated by Fe^{III}TSPP in weakly acidic media (pH = 5.81). The results, interpreted in Scheme 4, show that when the phosphine is the oxygen atom acceptor, the ferrous nitrosyl−porphyrin inter-

Table 2. Rate Constants for the Decomposition of Piloty's Acid Derivatives

product	rate constant (k, s^{-1})[a]	decomposition pH[b]	HNO donation pH[c]
Me−PA	$(1.91 \pm 0.09) \times 10^{-4}$	9	10.3
NO_2−PA	$(3.51 \pm 0.02) \times 10^{-4}$	5	5.5
F−PA	$(1.95 \pm 0.01) \times 10^{-3}$	3	3.8
Triiso−PA	$(4.97 \pm 0.02) \times 10^{-3}$	3	5.0
OMe−PA	$(3.53 \pm 0.07) \times 10^{-4}$	5	5.9
(NO_2−CF_3)−PA	$(6.32 \pm 0.08) \times 10^{-4}$	−1	*d*

[a]Rate constant at the decomposition pH. [b]pH at which decomposition starts to be observed by UV−visible or NMR spectroscopy. [c]Inflection point for the current vs pH curves. [d]Not measured.

mediate becomes protonated and releases HNO, generating an electrode signal.

Scheme 4. HNO Formation by Reaction of Fe(TSPP), Nitrite, and Phosphines (P)

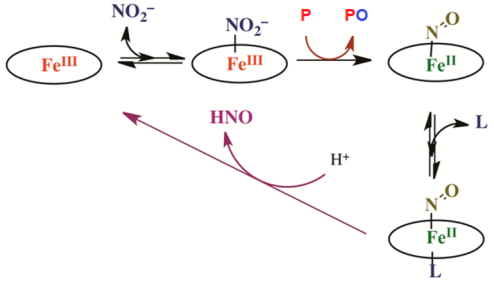

Interestingly, the presence of the phosphine is necessary for HNO production, since the use of thiol as oxygen acceptors shows neither any electrode signal nor N_2O production. Generation of HNO from nitrosyl porphyrins has not been reported previously under any circumstances. These results not only underscore the utility of the azanone sensing device for the elucidation of reaction mechanisms involving reactive nitrogen species, where HNO is a likely intermediate, but also draw our attention to the potential physiological production of azanone derived from protein based {FeNO}^{7} complexes, such as that proposed for the NOS enzyme.

The observation of HNO production from ferrous nitrosyl complexes, together with studies from Filipovic et al. showing

dx.doi.org/10.1021/ar500153c | *Acc. Chem. Res.* 2014, 47, 2907−2916

that both the soluble and iron coordinated "smallest" nitrosothiol HSNO, produced either through radical combination of NO and $HS^{\bullet}$ or H_2S and a pentacyano $\{FeNO\}^6$ complex, yield azanone,[5,49] prompted us to analyze the NO reaction with biologically compatible hydrogen atom donors and reductants in order to determine their possible role as chemical HNO sources.

Our results show that hydroxy/keto bearing reductants, such as ascorbic acid and hydroquinone, and phenolic compounds like the amino acid tyrosine react with NO in an effective bimolecular reaction to yield HNO (Scheme 5). This is shown

Scheme 5. Azanone Production through Indirect Hydrogen Atom Transfer to NO

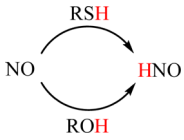

by the characteristic current vs time plot and NO/reductant concentration-dependent peak intensity determined with the HNO selective electrode. Mechanistic analysis combining EPR, MS, and DFT calculations strongly suggests that the reductants are able to produce HNO from NO through a mechanism involving indirect hydrogen atom transfer.

Related to the above mentioned results, we have recently shown, in collaboration with several groups, that NO reacts with H_2S at a fast rate by nucleophilic attack of HS^- to NO, yielding HNO (Scheme 5).[50] In this context, biological experiments showed that HNO is a potent activator of TRPA1 ion channel through the formation of disulfide bonds and that joint neuronal production of NO and H_2S results in channel activation. These data thus provide strong support of a chemical route to biological azanone production resulting in a specific physiological response.[50]

In summary, the presented examples show how the azanone selective electrode has become an invaluable tool to probe the chemical biology of HNO, allowing us to confirm its presence in several physiologically relevant reactions. These results, together with those of our colleagues,[49,51,52] emphasize the potential of reactions involving NO and HNO endogenous sources and make a strong case for further studies on their physiological effects, particularly in relation to the differences and similarities with those of NO and other potential biochemical azanone sources like NO_2^-, hydroxylamine, urea, cyanamide, etc.[1,53] Finally, although *in vivo* endogenous production of HNO has not been unequivocally established, the presented data suggest novel situations to be investigated.

SUMMARY AND PERSPECTIVES

After 10 years of research that began with the simple idea of producing ferrous nitrosyl complexes $\{FeNO\}^7$ through the reaction of ferric porphyrins with derived from spontaneous decomposition of its donors as an alternative to the more traditional route involving ferrous porphyrins and NO, we have traveled a path that has taken us through several (bio)inorganic research fields related to NO and HNO chemical biology. We have contributed to a deeper understanding of metal nitrosyl complexes, showing how the porphyrin substituents can stabilize extreme redox states like those of the $\{FeNO\}^8$ complexes, as well as characterizing the reactivity of Fe, Mn, and Co porphyrins with HNO and its donors, contributing also to their improvement and their versatility. Most importantly, all the knowledge gained from the studies of nitrosyl−metal-porphyrins has allowed us to develop a time-resolved HNO sensing device that, together with a battery of methods established in the past decade (Figure 1), has changed the paradigm of HNO chemistry and biology from a minor role of an elusive "NO-like" molecule to the center stage as a potential relevant intermediate in RNOS chemistry, a biological mediator, and a therapeutic agent. Fruits of this new-view are the central roles of HNO in several physiologically compatible reactions.

The future of HNO chemical biology is wide and deep; its role as chemical intermediate and its reactivity and end-products in many reactions are still not fully understood. Its biological role as a messenger molecule with its own pattern of effects in different physio- and pathological states is only beginning to emerge and is drawing the attention of an increasing number of biomedical researchers. Not to be forgotten is the potential involvement of HNO and both $\{FeHNO\}^8$ and $\{FeNO\}^8$ complexes in NO-reducing enzymes, including those related to the nitrogen cycle in the context of plants and microbial metabolism, a field that is as yet almost completely overlooked.[54] Lastly, the development of HNO donors as prodrugs requires as key evidence the detection of the active compound "HNO" *in vivo* at the site of action. Our electrode offers, in our view, the best perspective to become the reference method for these types of studies, and preliminary results show that it is able to detect azanone inside the left ventricle of a living rat after donor injection in a distant artery. This capability will be crucial in order to demonstrate HNO endogenous production and its biochemical role. Further research in this utmost relevant issue is ongoing and awaited with great expectations. The somewhat ignored brother of NO is growing and getting ready for the "big leagues".

AUTHOR INFORMATION

Corresponding Authors

*E-mail: doctorovich@qi.fcen.uba.ar.
*E-mail: marcelo@qi.fcen.uba.ar.

Notes

The authors declare no competing financial interest.

Biographies

Fabio Doctorovich was born in Buenos Aires, Argentina, in 1961. He received his Ph.D. degree from the University of Buenos Aires (UBA) in 1990. Following postdoctoral training at the Georgia Institute of Technology, he became Professor at the Department of Inorganic, Analytical and Physical Chemistry at UBA. In 2011, he was named a Fellow of the John Simon Guggenheim Memorial Foundation. His main research interests include investigations on NO and HNO chemistry, dealing with organic compounds, nitrosyl complexes, and metalloporphyrins.

Damian E. Bikiel was born in Buenos Aires, Argentina, in 1979. He received his Ph.D. in chemistry in 2009 at UBA. He has been involved in several different research areas ranging from quantum calculations of chemical reactions to organometallic synthesis of compounds and bioinorganic chemistry of CO, NO, and HNO. In 2014, he obtained the Molina Fellowship in Environmental Sciences and joined the Earth, Atmospheric and Planetary Science Department at MIT as Postdoctoral Fellow.

Juan Pellegrino was born in Buenos Aires, Argentina, in 1982. He received his Ph.D. in chemistry in 2013 at UBA. His doctoral thesis has focused on organometallic chemistry of NO complexes and bioinorganic chemistry of NO and HNO.

Sebastian A. Suarez was born in Buenos Aires, Argentina, in 1985. He obtained his M.Sc. in chemistry from UBA in 2011. He is currently completing his Ph.D. thesis studying the interaction of metalloporphyrins and heme proteins with nitroxyl, under the supervision of Doctorovich and Martí.

Marcelo A. Martí was born in Buenos Aires, Argentina, in 1979. He received his Ms.Sc. degree in Molecular biology in 2002 and Ph.D. degree in Chemistry in 2006 both from UBA, where he started the studies of HNO reactions with metalloporphyrins. In 2010, he became Professor at the Biological Chemistry Department (UBA). His main research interests include chemical biology studies of reactive nitrogen and oxygen species with metalloproteins combining experimental and computer simulation based approaches.

■ ACKNOWLEDGMENTS

The authors acknowledge ANPCyT, UBA, the John Simon Guggenheim Memorial Foundation, and CONICET for financial support. D.E.B., M.A.M., and F.D. are members of CONICET. Thanks to Benjamin Ridgway for proofreading.

■ REFERENCES

(1) Doctorovich, F.; Bikiel, D.; Pellegrino, J.; Suárez, S. A.; Larsen, A.; Martí, M. A. Nitroxyl (azanone) trapping by metalloporphyrins. *Coord. Chem. Rev.* **2011**, *255*, 2764−2784.

(2) Shafirovich, V.; Lymar, S. V. Nitroxyl and its anion in aqueous solutions: spin states, protic equilibria, and reactivities toward oxygen and nitric oxide. *Proc. Natl. Acad. Sci. U. S. A.* **2002**, *99*, 7340−7345.

(3) Paolocci, N.; Saavedra, W. F.; Miranda, K. M.; Martignani, C.; Isoda, T.; Hare, J. M.; Espey, M. G.; Fukuto, J. M.; Feelisch, M.; Wink, D. A.; Kass, D. A. Nitroxyl anion exerts redox-sensitive positive cardiac inotropy in vivo by calcitonin gene-related peptide signaling. *Proc. Natl. Acad. Sci. U. S. A.* **2001**, *98*, 10463−10468.

(4) Schmidt, H. H. H. W.; Hofmann, H.; Schindler, U.; Shutenko, Z. S.; Cunningham, D. D.; Feelisch, M. NO from NO synthase. *Proc. Natl. Acad. Sci. U. S. A.* **1996**, *93*, 14492−14497.

(5) Filipovic, M. R. M.; Miljkovic, J. L. J.; Nauser, T.; Royzen, M.; Klos, K.; Shubina, T.; Koppenol, W. H.; Lippard, S. J.; Ivanović-Burmazović, I.; Ivanovic, I. Chemical characterization of the smallest *S*-nitrosothiol, HSNO; cellular cross-talk of H_2S and *S*-nitrosothiols. *J. Am. Chem. Soc.* **2012**, *134*, 12016−12027.

(6) Bazylinski, D. A.; Hollocher, T. C. Metmyoglobin and methemoglobin as efficient traps for nitrosyl hydride (nitroxyl) in neutral aqueous solution. *J. Am. Chem. Soc.* **1985**, *107*, 7982−7986.

(7) Bazylinsky, D. A.; Goretski, J.; Hollocher, T. C. On the reaction of trioxodinitrate(II) with hemoglobin and myoglobin. *J. Am. Chem. Soc.* **1985**, *107*, 7986−7989.

(8) Kumar, M. R.; Pervitsky, D.; Chen, L.; Poulos, T.; Kundu, S.; Hargrove, M. S.; Rivera, E. J.; Diaz, A.; Colón, J. L.; Farmer, P. J. Nitrosyl hydride (HNO) as an O_2 analogue: Long-lived HNO adducts of ferrous globins. *Biochemistry* **2009**, *48*, 5018−5025.

(9) Bari, S. E.; Martí, M. A.; Amorebieta, V. T.; Estrin, D. A.; Doctorovich, F. Fast nitroxyl trapping by ferric porphyrins. *J. Am. Chem. Soc.* **2003**, *125*, 15272−15273.

(10) Martí, M. A; Bari, S. E.; Estrin, D. A.; Doctorovich, F. Discrimination of nitroxyl and nitric oxide by water-soluble Mn(III) porphyrins. *J. Am. Chem. Soc.* **2005**, *127*, 4680−4684.

(11) Suárez, S. A.; Martí, M. A.; De Biase, P. M.; Estrin, D. A.; Bari, S. E.; Doctorovich, F. HNO trapping and assisted decomposition of nitroxyl donors by ferric hemes. *Polyhedron.* **2007**, *26*, 4673−4679.

(12) Suárez, S. A.; Fonticelli, M. H.; Rubert, A. A; de la Llave, E.; Scherlis, D.; Salvarezza, R. C.; Martí, M. A; Doctorovich, F. A surface effect allows HNO/NO discrimination by a cobalt porphyrin bound to gold. *Inorg. Chem.* **2010**, *49*, 6955−6966.

(13) Roncaroli, F.; van Eldik, R. Mechanistic analysis of reductive nitrosylation on water-soluble cobalt(III)-porphyrins. *J. Am. Chem. Soc.* **2006**, *128*, 8042−8053.

(14) Boron, I.; Suárez, S. A.; Doctorovich, F.; Martí, M. A.; Bari, S. E. A protective protein matrix improves the discrimination of nitroxyl from nitric oxide by MnIII protoporphyrinate IX in aerobic media. *J. Inorg. Biochem.* **2011**, *105*, 1044−1049.

(15) Suárez, S.; Bikiel, D.; Wetzler, D.; Martí, M. A.; Doctorovich, F. Time-resolved electrochemical quantification of azanone (HNO) at low nanomolar level. *Anal. Chem.* **2013**, *85*, 10262−10269.

(16) Cline, M. R.; Tu, C.; Silverman, D. N.; Toscano, J. P. Detection of nitroxyl (HNO) by membrane inlet mass spectrometry. *Free Radical Biol. Med.* **2011**, *50*, 1274−1279.

(17) Reisz, J. A.; Zink, C. N.; King, S. B. Rapid and selective nitroxyl (HNO) trapping by phosphines: kinetics and new aqueous ligations for HNO detection and quantitation. *J. Am. Chem. Soc.* **2011**, *133*, 11675−11685.

(18) Donzelli, S.; Espey, M. G.; Flores-Santana, W.; Switzer, C. H.; Yeh, G. C.; Huang, J.; Stuehr, D. J.; King, S. B.; Miranda, K. M.; Wink, D. A. Generation of nitroxyl by heme protein-mediated peroxidation of hydroxylamine but not N-hydroxy-L-arginine. *Free Radical Biol. Med.* **2008**, *45*, 578−584.

(19) Dobmeier, K. P.; Riccio, D. A.; Schoenfisch, M. H. Xerogel optical sensor films for quantitative detection of nitroxyl. *Anal. Chem.* **2008**, *80*, 1247−1254.

(20) Rosenthal, J.; Lippard, S. J. Direct detection of nitroxyl in aqueous solution using a tripodal copper(II) BODIPY complex. *J. Am. Chem. Soc.* **2010**, *132*, 5536−5537.

(21) Zhou, Y.; Liu, K.; Li, J.-Y.; Fang, Y.; Zhao, T.-C.; Yao, C. Visualization of nitroxyl in living cells by a chelated copper(II) coumarin complex. *Org. Lett.* **2011**, *13*, 2357−2360.

(22) Shoeman, D. W.; Shirota, F. N.; DeMaster, E. G.; Nagasawa, H. T. Reaction of nitroxyl, an aldehyde dehydrogenase inhibitor, with N-acetyl-L-cysteine. *Alcohol.* **2000**, *20*, 55−59.

(23) Pino, R. Z.; Feelisch, M. Bioassay discrimination between nitric oxide (NO.) and nitroxyl (NO-) using L-cysteine. *Biochem. Biophys. Res. Commun.* **1994**, *201*, 54−62.

(24) Donzelli, S.; Espey, M. G.; Thomas, D. D.; Mancardi, D.; Tocchetti, C. G.; Ridnour, L. A.; Paolocci, N.; King, S. B.; Miranda, K. M.; Lazzarino, G.; Fukuto, J. M.; Wink, D. A. Discriminating formation of HNO from other reactive nitrogen oxide species. *Free Radical Biol. Med.* **2006**, *40*, 1056−1066.

(25) Tennyson, A. G.; Do, L.; Smith, R. C.; Lippard, S. J. Selective fluorescence detection of nitroxyl over nitric oxide in buffered aqueous solution using a conjugated metallopolymer. *Polyhedron* **2006**, *26*, 4625−4630.

(26) Samuni, U.; Samuni, Y.; Goldstein, S. On the distinction between nitroxyl and nitric oxide using nitronyl nitroxides. *J. Am. Chem. Soc.* **2010**, *132*, 8428−8432.

(27) Enemark, J. H.; Feltham, R. D. Principles of structure, bonding, and reactivity for metal nitrosyl complexes. *Coord. Chem. Rev.* **1974**, *13*, 339−406.

(28) Obayashi, E.; Takahashi, S.; Shiro, Y. Electronic structure of reaction intermediate of cytochrome P450nor in its nitric oxide reduction. *J. Am. Chem. Soc.* **1998**, *120*, 12964−12965.

(29) Lancon, D.; Kadish, K. M. Electrochemical and spectral characterization of iron mono- and dinitrosyl porphyrins. *J. Am. Chem. Soc.* **1983**, *105*, 5610−5617.

(30) Choi, I. K.; Liu, Y.; Feng, D.; Paeng, K. J.; Ryan, M. D. Electrochemical and spectroscopic studies of iron porphyrin nitrosyls and their reduction products. *Inorg. Chem.* **1991**, *30*, 1832−1839.

(31) Bykov, D.; Neese, F. J. Reductive activation of the heme iron-nitrosyl intermediate in the reaction mechanism of cytochrome c nitrite reductase: A theoretical study. *J. Biol. Inorg. Chem.* **2012**, *17*, 741−760.

(32) Pellegrino, J.; Bari, S. E.; Bikiel, D. E.; Doctorovich, F. Successful stabilization of the elusive species {FeNO}^{8} in a heme model. *J. Am. Chem. Soc.* **2010**, *132*, 989−995.
(33) Serres, R. G.; Grapperhaus, C. A.; Bothe, E.; Bill, E.; Weyhermüller, T.; Neese, F.; Wieghardt, K. Structural, spectroscopic, and computational study of an octahedral, non-heme [Fe-NO]$^{6-8}$ Series: [Fe(NO)(cyclam-ac)]$^{2+/+/0}$. *J. Am. Chem. Soc.* **2004**, *126*, 5138−5153.
(34) Speelman, A. L.; Lehnert, N. Characterization of a high-spin non-heme {FeNO}(8) complex: implications for the reactivity of iron nitroxyl species in biology. *Angew. Chem., Int. Ed.* **2013**, *52*, 12283−12287.
(35) Pellegrino, J.; Hübner, R.; Doctorovich, F.; Kaim, W. Spectroelectrochemical evidence for the nitrosyl redox siblings NO+, NO*, and NO- coordinated to a strongly electron-accepting Fe(II) porphyrin: DFT calculations suggest the presence of high-spin states after reduction of the Fe(II)-NO- complex. *Chem.—Eur. J.* **2011**, *17*, 7868−7874.
(36) Lee, J.; Richter-Addo, G. B. A nitrosyl hydride complex of a heme model [Ru(ttp)(HNO)(1-MeIm)] (ttp=tetratolylporphyrinato dianion). *J. Inorg. Biochem.* **2004**, *98*, 1247−1250.
(37) Lin, R.; Farmer, P. J. The HNO adduct of myoglobin: Synthesis and characterization. *J. Am. Chem. Soc.* **2000**, *122*, 2393−2394.
(38) Goodrich, L. E.; Roy, S.; Alp, E. E.; Zhao, J.; Hu, M. Y.; Lehnert, N. Electronic structure and biologically relevant reactivity of low-spin {FeNO}^{8} porphyrin model complexes: New insight from a bis-picket fence porphyrin. *Inorg. Chem.* **2013**, *52*, 7766−7780.
(39) Montenegro, A. C. A.; Amorebieta, V. T.; Slep, L. D.; Martín, D. F.; Murgida, D. H.; Bari, S. E.; Olabe, J. A. Three redox states of nitrosyl: NO+, NO., and NO−/HNO interconvert reversibly on the same pentacyanoferrate (II) platform. *Angew. Chem., Int. Ed.* **2009**, *48*, 4213−4216.
(40) Batinic-Haberle, I.; Spasojevic, I.; Tse, H.; Tovmasyan, A.; Rajic, Z.; St. Clair, D. K.; Vujaskovic, Z.; Dewhirst, M. W.; Piganelli, J. D. Design of Mn porphyrins for treating oxidative stress injuries and their redox-based regulation of cellular transcriptional activities. *Amino Acids* **2012**, *42*, 95−113.
(41) Álvarez, L.; Suarez, S. A.; Bikiel, D. E.; Reboucas, J. S.; Batinić-Haberle, I.; Martí, M. A.; Doctorovich, F. Redox potential determines the reaction mechanism of HNO donors with Mn and Fe porphyrins: defining the better traps. *Inorg. Chem.* **2014**, *53*, 7351−7360.
(42) Sharma, V. S.; Isaacson, R. A.; John, M. E.; Waterman, M. R.; Chevion, M. Reaction of nitric oxide with heme proteins: Studies on metmyoglobin, opossum methemoglobin, and microperoxidase. *Biochemistry* **1983**, *22*, 3897−3902.
(43) Laverman, L. E.; Ford, P. C. Mechanistic studies of nitric oxide reactions with water soluble iron(II), cobalt(II), and iron(III) porphyrin complexes in aqueous solutions: Implications for biological activity. *J. Am. Chem. Soc.* **2001**, *123*, 11614−11622.
(44) Miranda, K. M.; Paolocci, N.; Katori, T.; Thomas, D. D.; Ford, E.; Bartberger, M. D.; Espey, M. G.; Kass, D. A.; Feelisch, M.; Fukuto, J. M.; Wink, D. A. A biochemical rationale for the discrete behavior of nitroxyl and nitric oxide in the cardiovascular system. *Proc. Natl. Acad. Sci. U. S. A.* **2003**, *100*, 9196−9201.
(45) Sulc, F.; Immoos, C. E.; Pervitsky, D.; Farmer, P. J. Efficient trapping of HNO by deoxymyoglobin. *J. Am. Chem. Soc.* **2004**, *126*, 1096−1101.
(46) Scott, E. E.; Gibson, Q. H.; Olson, J. S. Mapping pathways for O2 entry and exit from myoglobin. *J. Biol. Chem.* **2001**, *276*, 5177−5188.
(47) Sirsalmath, K.; Suárez, S. A.; Bikiel, D. E.; Doctorovich, F. The pH of HNO donation is modulated by ring substituents in Piloty's acid derivatives: Azanone donors at biological pH. *J. Inorg. Biochem.* **2013**, *118*, 134−139.
(48) Heinecke, J. L.; Khin, C.; Pereira, J. C. M.; Suárez, S. A.; Iretskii, A. V.; Doctorovich, F.; Ford, P. C. Nitrite reduction mediated by heme models. Routes to NO and HNO? *J. Am. Chem. Soc.* **2013**, *135*, 4007−4017.
(49) Filipovic, M. R.; Eberhardt, M.; Prokopovic, V.; Mijuskovic, A.; Orescanin-Dusic, Z.; Reeh, P.; Ivanovic-Burmazovic, I. Beyond H2S and NO Interplay: Hydrogen Sulfide and Nitroprusside React Directly to Give Nitroxyl (HNO). A New Pharmacological Source of HNO. *J. Med. Chem.* **2013**, *56*, 1499−1508.
(50) Eberhardt, M.; Dux, M.; Namer, B.; Miljkovic, J.; Cordasic, N.; Will, C.; Kichko, T. I.; Roche, J. de la; Fischer, M.; Bikiel, D.; Suárez, S. A.; Dorsch, K.; Leffler, A.; Babes, A.; Lampert, A.; Lennerz, J. K.; Jacobi, J.; Martí, M. A.; Doctorovich, F.; Högestätt, E. D.; Zygmunt, P. M.; Ivanovic-Burmazovic, I.; Messlinger, K.; Reeh, P.; Filipovic, M. R. H2S and NO generate nitroxyl and activate HNO-trpa1-CGRP pathway for neurovascular control. *Nat. Commun.* **2014**, *5*, No. 4381.
(51) Heinecke, J.; Ford, P. C. Mechanistic studies of nitrite reactions with metalloproteins and models relevant to mammalian physiology. *Coord. Chem. Rev.* **2010**, *254*, 235−247.
(52) Switzer, C. H.; Miller, T. W.; Farmer, P. J.; Fukuto, J. M. Synthesis and characterization of lithium oxonitrate (LiNO). *J. Inorg. Biochem.* **2013**, *118*, 128−133.
(53) Fukuto, J. M.; Cisneros, C. J.; Kinkade, R. L. A comparison of the chemistry associated with the biological signaling and actions of nitroxyl (HNO) and nitric oxide (NO). *J. Inorg. Biochem.* **2013**, *118*, 201−208.
(54) Speelman, A. L.; Lehnert, N. Heme versus non-heme iron-nitroxyl {FeN(H)O}^{8} complexes: electronic structure and biologically relevant reactivity. *Acc. Chem. Res.* **2014**, *47*, 1106−1116.